Kramer's Escape Rate and Phase Transition Dynamics in AdS Black Holes with Dark Structures

Jafar Sadeghi ⋆[1], **Mohammad Ali S. Afshar** ⋆[2], **Saeed Noori Gashti**[†,⋆3], **Mohammad Reza Alipour** ⋆[4]

⋆Department of Physics, Faculty of Basic Sciences,
University of Mazandaran P. O. Box 47416-95447, Babolsar, Iran

†School of Physics, Damghan University, P. O. Box 3671641167, Damghan, Iran

Abstract

Traditional static methods in phase transition studies offer insights into black hole thermodynamics but miss dynamic aspects. Kramers' escape rate, central to our research, has a somewhat dynamic approach to phase transition. We explore free energy landscapes for black holes influenced by 'dark' and 'dark +strings' entities, assessing how additional parameters affect escape and transition rates during phase transitions from the small black holes to the large black holes. In our dual-perspective analysis, we first consider the escape rate as a function of the black hole radius, demonstrating a natural increase in the escape rate up to a Maximum point, followed by a decrease due to a reaction mechanism. From this viewpoint, the escape rate from smaller to larger black holes will consistently be greater than the reverse. From the second perspective, we consider the escape rate as a function of temperature (pressure). In both models under study, initially, the behavior of the probability diagrams is akin to the radius-based behavior. However, with an increase in temperature (and corresponding pressure), we reach a specific and distinct point, where the systems will move towards either smaller or larger black holes with the same probability. Beyond this temperature (pressure), the behavior of the models diverges. In the nonlinear model, an inversion occurs where the escape rate from larger black holes to smaller ones becomes predominant. This inversion area seems to be significantly reduced compared to the charged black hole model, although it is still discernible in the temperature-based escape rate diagram. In other words, within the temperature range studied, where the likelihood of radiative conditions and movement from a large black hole to a small black hole is less, It seems that the addition of dark parameters minimizes the occurrence of this transition, indicating the subtle influence of dark structures on the phase transition dynamics between black holes. In the string model, although the trend of increasing pressure in the transition from a large black hole to a smaller one is greater than the reverse, it seems that the transition process from a small black hole to a larger one, with decreasing pressure, completely prevents the 'low probable' transition from a large black hole to a smaller one. This is an interesting and distinctive observation.

Keywords: Phase Transition, Free Energy Landscape, Kramer's Escape Rate, Dark Structures.

[1]Email: pouriya@ipm.ir
[2]Email: m.a.s.afshar@gmail.com
[3]Email: saeed.noorigashti@stu.umz.ac.ir
[4]Email: mr.alipour@stu.umz.ac.ir

Contents

1 Introduction

From ancient times to the present, the existence of similar behavioral patterns and recurring elements in various physical systems, ranging from subatomic to cosmic scales, has been abundantly observed. This could be interpreted as a mysterious sign of a fractal structure inherent in the essence and fabric of nature. However, it can also be considered an intentionally hidden shortcut, ingeniously and knowingly embedded in the labyrinth of nature to guide us step by step in deciphering complexities that we cannot grasp all at once. Among the structures that have benefited most from the analogy of behavioral patterns for theoretical modeling, due to their inaccessibility for practical study, are black holes. The comparison of the gravitational field treatment of a black hole and its surrounding world, as a system and environment, with the behavior of a thermodynamic ensemble is indeed one of the most valuable achievements of this modeling. A resemblance that has led to black hole thermodynamics becoming a pioneering and fundamental branch in the evolution of our understanding not only of the structural nature of black holes, but also of the cosmos itself. If we were to highlight the three principal keys that paved the way for the application of thermodynamics and statistical mechanics to the study of black holes, we would undoubtedly mention Hawking temperature, Bekenstein-Hawking entropy, and the conversion of the cosmological constant to pressure. These concepts led to the formulation of the four fundamental laws of black hole thermodynamics [1–4]. With a slight indulgence, one might also add the exchange and conversion of enthalpy to mass to these golden keys [5].

The increasing study of black hole models based on thermodynamics and statistical mechanics has gradually revealed that, apparently, the best model that aligns most closely with current data and computational capabilities, and environmental conditions for studying black hole behavior, is the Van der Waals model (VdW). For instance, in canonical ensembles, a black hole phase transition was found in the background of charged rotating AdS black holes, reminiscent of the liquid-to-gas phase transition of the (VdW) fluid [6–8]. It was also observed that there is a significant resemblance between the (VdW) liquid-gas system and the charged black hole in the extended phase space [9, 10], or another study showed the critical behavior of charged black hole in fixed charge ensemble coincides exactly with that of (VdW) liquid-gas system [11]. Undoubtedly, phase transition is one of the most fundamental phenomena in classical thermodynamics, which, through extensive study of various structures of matter, has led to a profound understanding of the true behavior of systems in the past. The question that quickly arose was whether, given the (VdW)-like thermodynamic behavior of black holes, these structures, considering their quantum-relativistic structural pattern, could exhibit quasi-material behavior and phase transitions. And if so, what could be the cause of the initiation of this process? The answer to the first part of the question was subsequently obtained, as it was determined that there exists a Hawking-Page phase transition between a large stable black hole and pure thermal radiation [12]. Of course, numerous other studies were conducted that even confirmed the interesting phase transition behaviors for black holes [13–28]. However, the second part of the question remains unclear to us until now.

Although the temperature variation graph of a system can itself be a reliable criterion for phase transition detection, one of the tools that can be used to study the behavioral range of thermodynamic phase transition with greater precision is the free energy landscape. Free energy landscape provides a way to visualize and understand how systems, transition between different states over time. The dependence of free energy on temperature causes temperature changes to significantly alter the free energy landscape. Consequently, studying these apparent changes can provide a better understanding of the system's behavior and the formation of transitions between different phase states. In thermodynamics, free energy is rewritten in various forms depending on the system's conditions. However, since the interplay between temperature and pressure is often of primary concern in black hole structures, and since enthalpy offers a better and simpler description of energy transfer at a specific pressure, the Gibbs free energy function is a better candidate among the various definitions of free energy for studying black holes. But the point that was hidden in the study of the phase transition behavior of black holes using Gibbs free energy was that, apparently, in this form of study, no attention was paid to the rate and mode of transition from one state to another. In other words, in these studies, we did not address the following points in the phase transition process from small to large black holes:

- At what rate do these processes occur?
- Is the rate of transition constant across different temperature ranges?
- Does the initial state (small black hole) completely vanish at the end of the transition?

Also, could there be hidden points in the leakage from the small to the large black hole that we are unaware of? These and similar questions that address the dynamics of phase transitions provide important information about the phase transitions of black holes, which apparently cannot be obtained in the initial analyses of Gibbs free energy. It seems that we were considering the phase transition and its results in a static manner, only at the end points and equilibrium points of Gibbs. Recent studies have observed that phase transition under thermal fluctuations can be examined through the Fokker-Planck equation in non-equilibrium physics, based on the free energy landscape, particularly the Gibbs form. Accordingly, it has been observed that in black holes, a transition occurs from small to large black holes and vice versa, influenced by temperature and the height of the potential barrier in the free energy landscape [29–32]. According to the studies done, it seemed that the Gibbs free energy is in the form of an effective potential it plays the role of a driving force that leads to the phase transition of the black hole [33]. Based on this, a special focus was formed on the Gibbs energy landscape, which, according to the structure of the Fokker-Planck equation, tried to investigate some kinetics of the phase transition by calculating the mean first passage time in several black holes [34–56]. Of course, other efforts were also made in this direction based on the rewriting of free energy in terms of Landau free energy [57,58] or thermal potential [59–62].

One might pose the question: How has the connection between stochastic-form equations and phase transitions, as well as thermodynamic equations, been established? In response, it should be noted that since some thermodynamic processes in the system are driven by stochastic fluctuations, it would be logical to employ the method of analyzing non-equilibrium stochastic processes to study the occurrence of inherently non-equilibrium thermodynamic processes. Building on this foundation, in this paper, we consider two black holes influenced by dark energy, namely:

- Non-Linear Magnetic-Charged AdS black hole surrounded by Quintessence, in the background of Perfect Fluid Dark matter (NLM-C-Q-PFD) [63].
- 4D AdS Einstein-Gauss-Bonnet-Yang-Mills Black hole with a Cloud of Strings (EGB-YM-CS) [64].

Initially, we calculate the various forms of free energy mentioned and demonstrate that all three forms will exhibit nearly identical behavior in the canonical ensemble. Subsequently, using Kramer's escape rate method, we will examine the characteristics of their first-order phase transition rate in terms of variations in radius, pressure, or temperature. We will then compare our results with those of black holes studied using the same method [59–62] to determine the influence of the added parameters.

The present paper is organized as follows: In Section 2, we explore the theoretical preliminaries to thoroughly study and introduce various concepts, such as Kramer's escape rate and different forms of the free energy landscape. This includes the Gibbs free energy landscape, Landau free energy, and thermal potential. In Section 3, we conduct a behavioral comparison of the free energy landscape and Kramer's escape rate for (NLM-C-Q-PFD) AdS black hole. Section 4 presents an accurate calculation for the (NLM-C-Q-PFD) AdS black hole. In Section 5, we fully analyze the concepts discussed in the previous two sections. Finally, in Section 6, we comprehensively present the results of our work.

2 Theoretical preliminaris

2.1 Kramer's escape rate

The study of Brownian particle leakage or escape under thermal fluctuations from a stable or metastable potential, known as the Kramers problem, is a fascinating topic that has garnered attention across most branches of physics [62]. This subject, in addition to the diverse results it has yielded throughout its study, has led to the calculation of a relationship known as the Kramers escape rate. We will briefly address this for a better understanding here. As we can see in Fig (1), the point x_{min} is a local minimum such that particles are in equilibrium

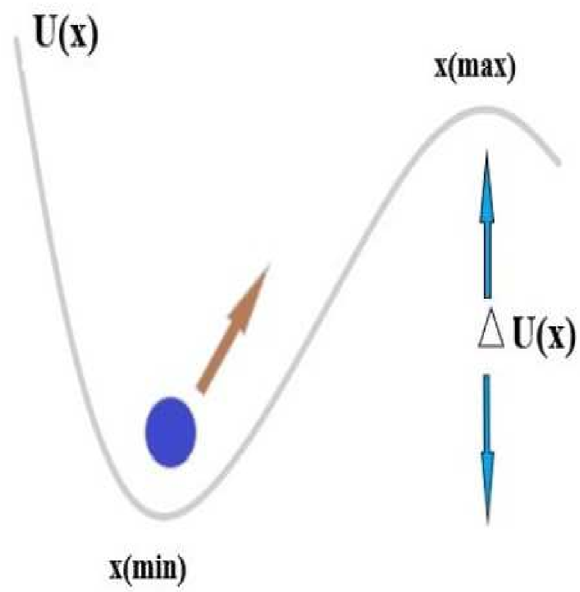

Figure 1: The possibility of leakage due to Brownian motion or thermal fluctuation

at this point and maintain their original position under small perturbations. Without loss of generality and for simplicity, we can point out a few things here. For instance, we assume only one direction of escape, which may occur through the nearest local maximum located at x_{max}. On the left side of x_{min}, the potential is such that it does not have any additional extremes. After the local maximum at x_{max}, on the right side, there may be another local or global minimum, or even the potential may be unbounded below, which is irrelevant. This is because the escape rate should be independent of the shape of the potential on the right side of x_{max}. When we add the effect of thermal baths to the system, the particles are affected by the two competing effects of fluctuation and dissipation. Random forces arising from thermal fluctuations push the particle away from its initial position and allow it to eventually climb the potential barrier. On the other hand, damping tends to slow the particle down and makes it more difficult to return to the equilibrium point. There are three possible situations here.

• Very Low Damping: In this scenario, particles experience minimal frictional forces. The escape rate is determined by the energy diffusion regime, where the particle's inertia plays a significant role. The particle can oscillate many times near the potential well's boundary before escaping, and the escape rate is relatively low due to the lack of significant damping forces.
• Intermediate Damping: The escape rate in this regime is more complex to describe, as it involves a balance between inertial effects and damping forces. The system oscillates less than before, but it can still exist, and the escape rate is still not significant.
• Over-damped: In the over-damped case, the damping forces are strong, and the system experiences high frictional forces, which dominate over inertial effects. The particle moves slowly away from the potential well, and the escape rate is governed by the rate at which the system can overcome the barrier height compared to the thermal energy. The escape process is akin to a slow, diffusive motion over the barrier, and the escape rate is higher than in the very low or Intermediate damping case and is significant.
Since we intend to simulate this model according to the phase transition behavior of the black hole, then among the above options, the over-damping mode seems to be the appropriate option, since due to the strengthening of the combined effect in this mode, the system is no longer stable and The probability of the particle exiting the well will start to grow. That is, after a sufficient period of time, we can expect the particle to have almost passed through the barrier. The escape rate is closely related to the inverse of the average time required for the first passage of the local maximum potential, which is called the "mean first passage time", which was noted in articles [35–56]. It should be noted that the escape rate is different from the diffusion rate to the next minimum [65–70].
Let us consider the the Fokker-Planck equation [67, 70, 71],

$$\frac{\partial}{\partial t}P(x,t) = -\frac{\partial}{\partial x}J(x,t)\,,$$

where the $P(x,t)$ is the probability distribution of particles and current J is defined as,

$$J = -\frac{\left(\frac{\partial}{\partial x}U(x,t)\right)P(x,t)}{\gamma} - \mathrm{D}\left(\frac{\partial}{\partial x}P(x,t)\right),$$

here $U(x)$ is a potential field, γ is the friction coefficient and D is the diffusion coefficient. The current can be rewritten as follows,

$$J = -\mathrm{D}\mathrm{e}^{-\frac{U}{k_BT}}\frac{\partial}{\partial x}(\mathrm{e}^{-\frac{U}{k_BT}}P),$$

k_B is the Boltzmann constant and T is the temperature. To integrate, we rewrite the above relation as follows,

$$\frac{\partial}{\partial x}(\mathrm{e}^{-\frac{U}{k_BT}}P) = -\frac{J\mathrm{e}^{\frac{U}{k_BT}}}{\mathrm{D}}.$$

By integrating from the above equation and taking into account the fact that on the left side of the equation, the contribution of the distribution term P in x_{min} dominates over x_{max}, we can conclude,

$$J = \frac{\mathrm{D}\mathrm{e}^{\frac{U(x_{\min})}{k_BT}}P(x_{\min})}{\int_{x_{\min}}^{x}\mathrm{e}^{-\frac{U(x)}{k_BT}}dx}.$$

Now, if we consider the upper limit of the integral of the denominator in the above equation at a point on the right side of x_{max} and using the expansion around x_{max} and after some calculations, we will have,

$$\int_{x_{\min}}^{x} \mathrm{e}^{-\frac{U(x)}{k_B T}} dx = \sqrt{\frac{2\pi k_B T}{|\frac{d^2}{dx^2} U(x_{max})|}}\, \mathrm{e}^{\frac{U(x_{\max})}{k_B T}}.$$

If we define p as the probability of the particle being inside the well, then with some calculations we can find that,

$$p = P(x_{\min}) \sqrt{\frac{2\pi k_B T}{|\frac{d^2}{dx^2} U(x_{min})|(x)\,|}}.$$

Finally, using the definition of Kramers escape rate($r_k = J/P$), we will have,

$$r_k = \frac{\mathrm{D}\sqrt{|\frac{d^2}{dx^2} U(x_{max})\frac{d^2}{dx^2} U(x_{min})|}\, \mathrm{e}^{-\frac{U(x_{\max})-U(x_{\min})}{k_B T}}}{2\pi k_B T}.$$

When the system reaches thermal equilibrium, D can be considered constant[55], and with a little simplification, the above relationship can be rewritten as follows[56],

$$r_k = \frac{\sqrt{|\frac{d^2}{dx^2} U(x_{max})\frac{d^2}{dx^2} U(x_{min})|}\, \mathrm{e}^{-\frac{U(x_{\max})-U(x_{\min})}{D}}}{2\pi}. \tag{1}$$

Note that the formula can only be applied for $\Delta U >> k_B T$.

2.2 Different shapes for free energy landscape

Free energy landscape provides a way to visualize and understand how systems, transition between different states over time. In simple terms, the free energy landscape is a graphical representation where each point on the landscape corresponds to a possible state of the system. From the vantage point of free energy, the exploration of phase transition conditions becomes accessible through the scrutiny of the emergence and stability of distinct phases. Furthermore, the characterization and analysis of the free energy landscape are profoundly influenced by its relationship with the order parameters. Taking the radius of a black hole's event horizon as an exemplary order parameter, one can articulate the free energy landscape. Consequently, the phase transition of a black hole can be interpreted as a stochastic thermal fluctuation of said order parameter, offering a novel perspective on the underlying physics [33]. In the following, since we want to study the phase transition from the perspective of the free energy landscape and in a different structure under specific thermal fluctuations, we will introduce different forms of this energy that can help us in this way.

2.2.1 Gibbs Free Energy Landscape

The Gibbs free energy function, renowned for its intrinsic reliance on enthalpy and temperature, emerges as the special tool for probing the phase transitions within a black hole's architecture, particularly under constant pressure conditions. The swallowtail behavior, manifested graphically as a function of temperature, stands as a prevalent methodology for the exploration of phase transitions. Within the formalism of the free energy perspective, the Gibbs free energy is delineated as a continuous function that is intimately connected to the system's order parameter, thereby providing a robust framework for the analysis of phase behavior,

$$G = H - T_H S, \tag{2}$$

which T_H is Hawking temperature, H is enthalpy and S is entropy. Also considering the correspondence between mass and enthalpy in the extended phase of a black hole ($H \equiv M$), this equation can be rewritten in terms of mass.

During the intricate process of phase transition, particularly of the first order, an assortment of black holes of varying sizes-small, medium, and large-along with transitional states, frequently emerges. Consequently, it is feasible to conceptualize a collection of these black hole space-times, each with an arbitrary horizon radius, at a specified temperature "T". For a better understanding, it must be stated that one of the most important characteristics of a black hole is its temperature, or more specifically, the Hawking temperature. The mere existence of temperature, regardless of how it is defined, implies the possibility of thermal fluctuations within the system. Consider this as a background. Now, the black hole under study has been excited for some environmental reason and begins a phase transition process. At both the initial and ends of this phase transition, there are two locally stable black holes, one of which is globally more stable than the other, setting the stage for this transition. However, an important point regarding these two states is that both must necessarily be solutions to Einstein's field equations. The golden key to defining a set of black holes lies here. Although the system must end up in a state that is necessarily a solution to Einstein's equations at both ends, there is no need to strictly follow the static field equations during the transition from the initial phase to the final phase, since the system is in an unstable transitional phase. Therefore, considering a predefined energy range and with the condition that the chosen paths do not destroy the overall stability of the system, the system can be allowed to traverse any desired path from the origin to the end. This freedom of choice and multiple paths could serve as a gateway for the introduction of probability and statistical methods. Hence, by selecting an arbitrary indistinctive set within this framework, which acts as a canonical ensemble for us, a statistical framework for analysis can be presented. It is noteworthy that the temperature "T" of the ensemble may differ from the Hawking temperature associated with black holes Notably, the temperature "T" of the ensemble may diverge from the Hawking temperature associated with black holes. Each of the space-time configurations within this ensemble is characterized by a distinct Gibbs free energy. Hence, we refer to this construct as the generalized Gibbs result or, more descriptively, the Gibbs free energy landscape.

$$G_L = M - TS. \tag{3}$$

The terminology 'on-shell' and 'off-shell' delineates the aforementioned temperature discrepancy. 'Off-shell' encompasses all transitions occurring at temperature "T", which, despite conforming to the laws of thermodynamics, do not necessarily constitute solutions to Einstein's field equations [33]. It is imperative to recognize that solely the extremal points on the G_L signify the authentic black hole phases that comply with the Einstein field equations. Furthermore, within this context, the local maxima and minima are indicative of the unstable and locally stable black hole phases, respectively [72].

2.2.2 Landau free energy

The Landau free energy constitutes another showy path for scrutinizing the phase transition dynamics within the system's free energy landscape. While using this method assumes heightened significance in the context of second-order phase transitions- wherein the bifurcation of the Landau functional's local minimum epitomizes the thermodynamic system's second-order phase transition- it is also pertinent to first-order phase transitions. Specifically, the transmutation of the global minimum is emblematic of a first-order phase transition, underscoring the multifaceted nature of the Landau-free energy in characterizing phase behavior. This function can be written as follows, [57]

$$L = \int F(X, P, T)\, dX, \tag{4}$$

that in the delineated relationship, P denotes pressure, T represents temperature, and X serves as an auxiliary variable. However, in the realm of black hole thermodynamics, pressure holds a distinctive advantage. Contrary to other thermodynamic variables such as temperature, mass, and volume -which are solely functions of the event horizon's radius- pressure not only contributes to the equation of state, inextricably linked to the radius, but also assumes an independent role based on the definition of the cosmic constant in the studied model. This endows it with a unique identity within the thermodynamic landscape. Consequently, preserving the essence of generality, the "F" function can be reformulated as follows,

$$F(X, P, T) = P - f(X, T)\,. \tag{5}$$

Given that "L" is an energy function, it inherently embodies the fundamental characteristic of energy minimization. This implies that the system invariably seeks a trajectory that reduces the energy expenditure required for transformation. Therefore, among the triad of system parameters (X, P, T) that influence the "F" function, only the configurations that minimize "L" will accurately reflect the system's state.

$$\frac{d}{dX}L \;= F(X, P, T) = 0. \tag{6}$$

The important point before the end of this section is that the most familiar form of the characteristic "X" in Landau's definition is the volume, to be able to use the probabilistic method for this function, we must consider the volume off-shell

2.2.3 Thermal potential

Another form of landscape energy that can be used to investigate phase transition based on thermal fluctuation is the model that was introduced in [59] under the title of thermal potential.

$$U = \int (T_H \;- T\;)\, dS, \tag{7}$$

which T_H is Hawking temperature,T is 'Off-shell' temperature, and S is entropy that has appeared here in the role of a variable. Since In thermodynamics, the vigor of thermal motion is quantified by the product of temperature and entropy. Consequently, the aforementioned thermal potential serves as an approximate gauge for the extent to which all conceivable states within the canonical ensemble deviate from the genuine black hole state.
When a black hole system is situated within a potential field U, it is subject to thermodynamic fluctuations. The resultant stochastic behavior of black holes within such a potential field can offer insights into certain thermodynamic attributes of black holes. Furthermore, the thermal potential's utility extends to its ability to indicate system stability through the analysis of concavity and convexity at critical points.

3 Non-linear magnetic-charged AdS black hole surrounded by quintessence in the perfect fluid dark matter background

In this article, we went to black holes that somehow interact with the structure of matter and dark energy, so that we can study the effect of the presence of parameters caused by the dark structure on the first-order phase transition. So the metric of (NLM-C-Q-PFD) black holeis as follows [63],

$$f(r) = 1 - \frac{2M\,r^2}{Q^3 + r^3} + \frac{\alpha \ln\left(\frac{r}{|\alpha|}\right)}{r} - \frac{c_q}{r^{3\varepsilon+1}} + \frac{8\pi P\,r^2}{3}.$$

For the main quantities of this model i.e. mass M, Hawking temperature T_H, entropy S, pressure P and volume V we will have (note that as long as there is no specific definition of the radius, it will be $r = r_H$ in calculations) [63],

$$M = \frac{\left(Q^3 + r^3\right)\left(1 + \frac{\alpha \ln\left(\frac{r}{|\alpha|}\right)}{r} - \frac{c_q}{r^{3\varepsilon+1}} + \frac{8\pi P\,r^2}{3}\right)}{2r^2}, \tag{8}$$

$$T_H = \frac{\frac{-2Q^3+r^3}{r} + \frac{3c_q\varepsilon\left(r^3+\frac{Q^3(\varepsilon+1)}{\varepsilon}\right)}{r^{3\varepsilon+2}} + \frac{\alpha Q^3\left(1-3\ln\left(\frac{r}{|\alpha|}\right)\right)}{r^2} + \alpha r + 8\pi P\,r^4}{4\pi\left(Q^3 + r^3\right)}, \tag{9}$$

$$S = \pi r^2\left(1 - \frac{2Q^3}{r^3}\right), \tag{10}$$

$$P = \frac{3\alpha Q^3 \ln\left(\frac{r}{|\alpha|}\right) - 3r^{3-3\varepsilon}c_q\varepsilon - 3Q^3 c_q\left(\varepsilon+1\right)r^{-3\varepsilon} + \left(4\pi T\,r^2 - \alpha + 2r\right)Q^3 + 4T\pi r^5 - r^4 - \alpha r^3}{8\pi r^6}, \tag{11}$$

$$V = \frac{4\pi\left(Q^3 + r^3\right)}{3}, \tag{12}$$

where α denotes the intensity of the PFDM, c_q and ε are the quintessence parameters and Q is the magnetic charge.

3.0.1 Behavioral comparison of landscape free energy

Now according to equations (2), (3), (4) and (7) for Gibbs and Landau free energy function and also the thermal potential of this model, we will have,

$$\begin{aligned}
&\mathbf{G} = \mathcal{A} + \mathcal{B},\\
&\mathcal{A} = \frac{\left(Q^3 + r^3\right)\left(3r + 3\alpha\ln\left(\frac{r}{|\alpha|}\right) - 3c_q r^{-1-3\varepsilon} r + 8\pi P r^3\right)}{6r^3}\\
&\mathcal{B} = \frac{\left(-\frac{2Q^3 - r^3}{r} + 3c_q\left(Q^3\varepsilon + r^3\varepsilon + Q^3\right) r^{-2-3\varepsilon} + \frac{\alpha Q^3\left(1 - 3\ln\left(\frac{r}{|\alpha|}\right)\right)}{r^2} + \alpha r + 8\pi P r^4\right)\left(2Q^3 - r^3\right)}{4r\left(Q^3 + r^3\right)}
\end{aligned} \tag{13}$$

$$G_L = \frac{\left(Q^3 + r^3\right)\left(1 + \frac{\alpha\ln\left(\frac{r}{|\alpha|}\right)}{r} - \frac{c_q}{r^{1+3\varepsilon}} + \frac{8\pi P r^2}{3}\right)}{2r^2} - T\pi r^2\left(1 - \frac{2Q^3}{r^3}\right) \tag{14}$$

$$\begin{aligned}
&\mathbf{L} = PX - \frac{\mathcal{C} + \mathrm{D}}{48Q^3\pi^2 - 36\pi X},\\
&\mathcal{C} = 36\left(Q^3\pi^{\frac{7}{3}} - \frac{\pi^{\frac{4}{3}}X}{4}\right)2^{\frac{2}{3}}T\left(-4\pi Q^3 + 3X\right)^{\frac{2}{3}} + 9\,2^{\frac{1}{3}}X\pi^{\frac{2}{3}}\left(-4\pi Q^3 + 3X\right)^{\frac{1}{3}},\\
&\mathrm{D} = 6\ln\left(-4\pi Q^3 + 3X\right)\pi X\alpha - 18X\pi^{\varepsilon+1}c_q\left(-\pi Q^3 + \frac{3X}{4}\right)^{-\varepsilon} - 8Q^3\pi^2\alpha\left(\ln(\pi) + 3\ln(|\alpha|) + 2\ln(2)\right),
\end{aligned} \tag{15}$$

$$\begin{aligned}
&\mathbf{U} = \mathcal{E} - T\pi r^2\left(1 - \frac{2Q^3}{r^3}\right),\\
&\mathcal{E} = \frac{3c_q\left(-Q^3 - r^3\right) r^{-3\varepsilon} + 3\alpha\left(Q^3 + r^3\right)\ln(r) + 8\pi P r^6 - 3\alpha Q^3\ln(|\alpha|) + 3Q^3 r + 3r^4}{6r^3}
\end{aligned} \tag{16}$$

.

Now we will go to a special state that is formed based on the arbitrary parameter setting. For this purpose, by considering the values $\alpha = 0.6, c_q = 0.2, \varepsilon = -2/3, Q = 1$ for the parameters and with a little calculation for the critical quantities, we will have,

$$\begin{aligned}
&T_c = 0.02426755451, \quad P_c = 0.00456781599, \quad r_c = 2.594697206,\\
&V_c = 77.36141969, \quad U_c = 1.00399626317, \quad G_c = 1.02312988617.
\end{aligned} \tag{17}$$

According to the usual procedure, we convert the parameters into dimensionless form so that the results can be compared with other studies in addition to convenience,

$$t = \frac{T}{T_c}, \quad p = \frac{P}{P_c}, \quad x = \frac{r}{r_c}, \quad \widetilde{G} = \frac{G}{G_c}, \quad \widetilde{G}_L = \frac{G_L}{G_c}, \quad l = \frac{L}{G_c}, \quad u = \frac{U}{U_c}. \tag{18}$$

Before any calculations, it is better first compare the various forms of free energy definitions, namely G_L, U, and L. Theoretically, from the canonical perspective the number of particles and mass should remain constant, consequently only the entropy-temperature and pressure-volume terms will play a role in the first law of thermodynamics. Additionally, given that in Landau's free energy, X can be considered equivalent to volume, it appears that ultimately, all three introduced forms for the free energy landscape must coincide. In Fig (2a) and (2b), for the model under study, we have plotted these three definitions once according to their general structure and once based on their dimensionless state. Practically, in terms of the shape structure, all three forms have the same trend, but there are also some visible differences, some of which may be attributed to computational precision. Moreover, since Landau's free energy has dimensions of energy, we used the G_c to render it dimensionless, which seems to have increased the degree of displacement, although the shape has been preserved. An intriguing point that comes to mind before concluding this discussion is that in statistical ensembles, such as the grand canonical ensemble where terms related to the chemical potential play a more prominent role, the complexities and structural differences of these three definitions may become more apparent compared to this scenario. Concerning the above discussion and as seen in Fig (2), all the shapes of the free energy landscape (with a little tolerance for displacement) will practically have the same shape structure in the canonical view. Accordingly, the choice and use of each do not seem to have an advantage over the others. For this reason, we will henceforth utilize them under the designation of the free energy landscape, without loss of generality. Now, to be able to interpret

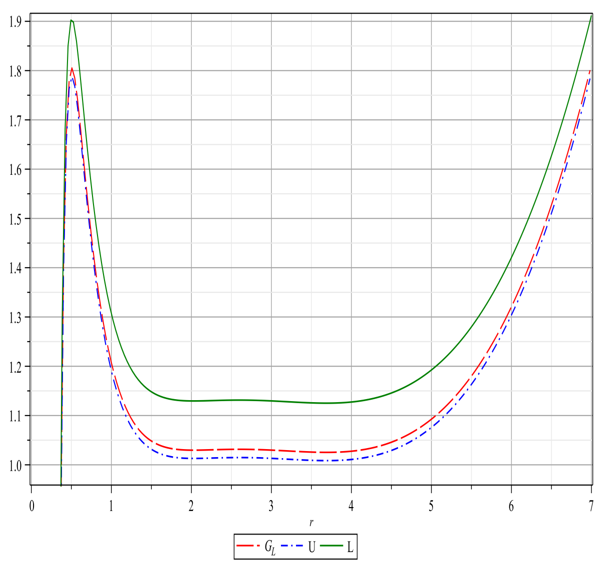

(a)

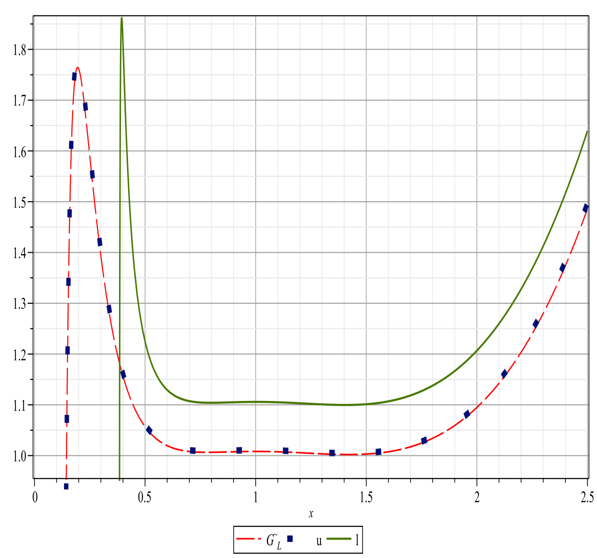

(b)

Figure 2: Comparison of the Gibbs landscape free energy (G_L), thermal potential (U), and Landau free energy (L) in the diagram in two states, i.e., with dimension in fig (2a) and dimensionless in fig (2b)

the behavior of the energy function, we need to have the graph of temperature changes Fig (3a) and Gibbs free energy in terms of temperature Fig (3b).

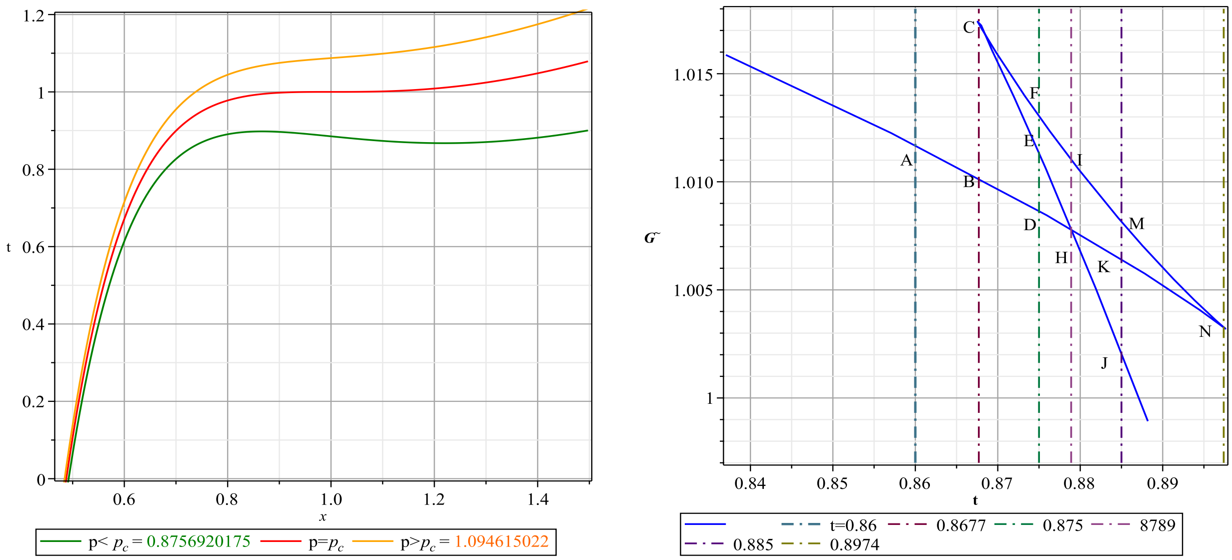

(a) (b)

Figure 3: The graph of T against x for free parameters in fig (3a) and Gibbs Free energy versus temperature in fig (3b)

To better interpret the behavior of free energy, we initially turn to the swallowtail fig (3b). In this figure, the line (A-N) represents the small black hole, and(C-J) represents the large black hole, both of which are locally stable with positive heat capacity, and the line (N-C) with negative heat capacity represents the intermediate black hole, which is unstable. As a classical principle, we know that systems always tend to choose states with the least amount of energy. This principle also holds for the free energy landscape, meaning the system will move towards its minimum. In other words, the minima of the energy function correspond to stable states, and its maxima represent unstable states. Considering the overall shape in Fig (4), it is also important to note that in a system with multiple local minima, each of these minima, although locally stable relative to their immediate vicinity, may act as unstable states globally relative to the primary minimum. Even if the system is initially in these states, over time it will progress towards the ultimate global minimum.

In Fig (4a), as is evident, the potential at point A has a global minimum, which belongs to the branch of the small black hole. Over time, with the increase in temperature, in Fig (4b), the local extrema B (minimum) and C (maximum) begin to form. However, they are still in the form of globally unstable states, and the system tends to maintain its position at the primary minimum on the branch of the small black hole. The situation in Fig (4c) is similar to (4b), with the difference that the local extrema have fully formed. With a gradual increase in temperature, the system progresses towards the formation of a large and stable black hole, as shown in Fig (4d). Yet, the small black hole also exists in a stable state, indicating a situation where two equivalent global minima are created. This state corresponds to the isotherm line (H-I) in Fig (3b), which seemingly has a maximum on the branch of the intermediate black hole (I) and a global minimum (H). However, in reality, (H) is located on both the small and large black holes, meaning that a state is created where both the small and large black holes appear simultaneously and stably. In other words, a coexistence phase between the two stable black holes is formed. Further, the process of temperature increase will strengthen the large black hole and weaken the small black hole, Fig(4e) and (4f). The point that can be mentioned at the end of this discussion is related to the second-order phase transition. When we study the system at a temperature higher than the critical temperature, Fig(4g), the system will follow a path similar to (I-H-J) in Fig (3b), and practically it is directly and continuously transferred from the small black hole to the large one.

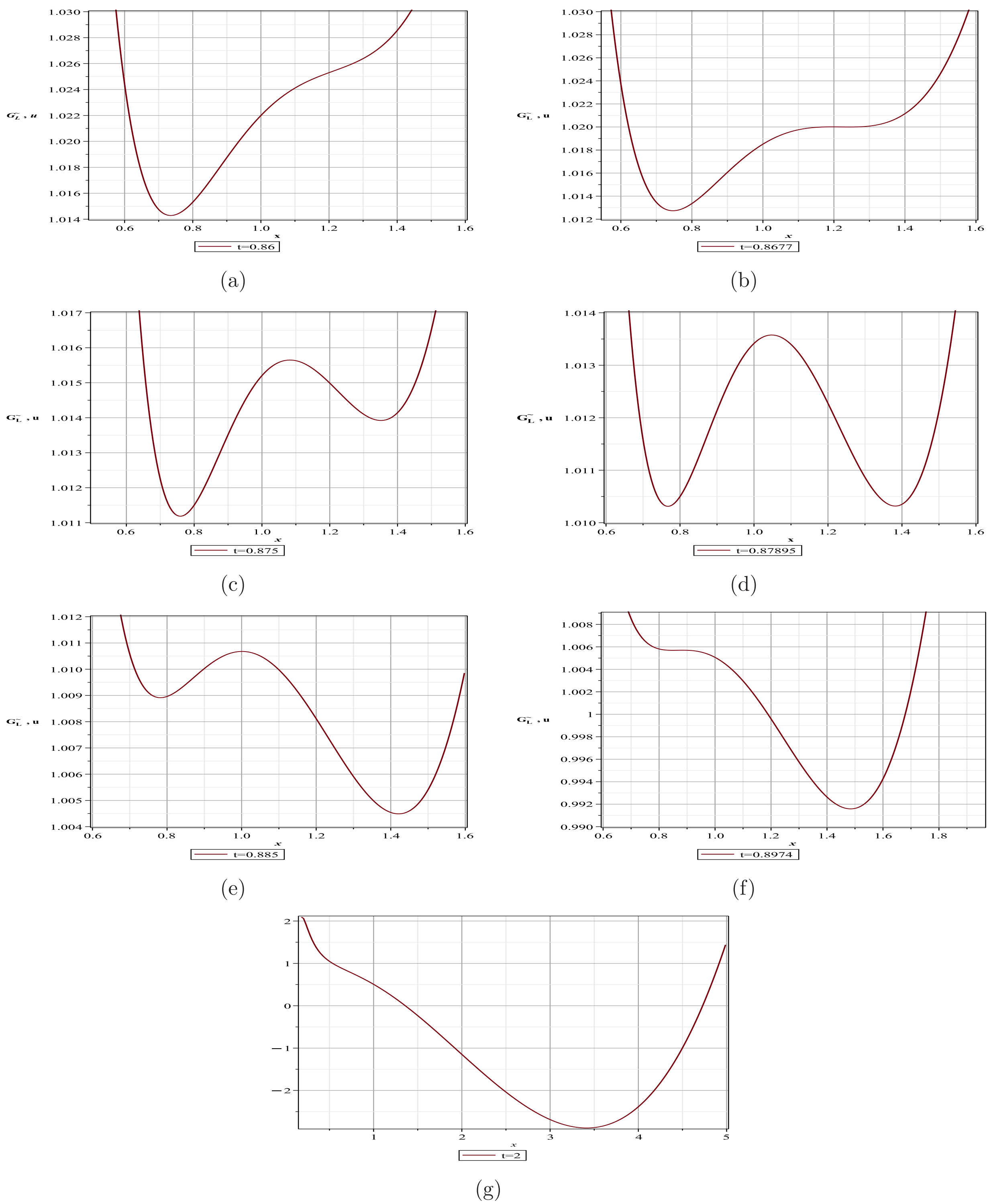

Figure 4: Behavioral sequence of energy in terms of x for different temperatures

3.0.2 Kramer's escape rate

An important point to focus on initially is the difference in concept between this section and the previous one. Contrary to the previous section, here we do not intend to study the influence of temperature on free energy and the process of transition from a small to a large black hole during a first-order phase transition. Instead, we aim to examine, in light of the concepts previously discussed for Kramer's escape rate -which represents the rate of particle escape under thermal fluctuations from a known local minimum in the potential- whether conditions might arise that could reverse the transition process from a small to a large black hole? Typically, we expect a transition from an unstable local minimum to a stable global minimum. However, the question arises whether there is a range in which, due to environmental conditions such as changes in temperature or pressure, the probability of a reverse process, namely the transition from a large to a small black hole, could precede the primary and natural process, causing systems to move in reverse from the large to the small black hole. To better understand, Fig (5a) illustrates a specific instance of a free energy landscape at a defined pressure of $p = 0.875692$. For this particular scenario, we examine two states:

1. The investigation of leakage or the probability of transition from the unstable local minimum alpha to the stable global minimum gamma, which is conventionally expected to occur with an increase in temperature.
2. The examination of the likelihood that, under certain environmental conditions such as increased temperature or pressure, the reverse process, namely the transition from gamma to alpha, could become the dominant process, even if only in a small region.

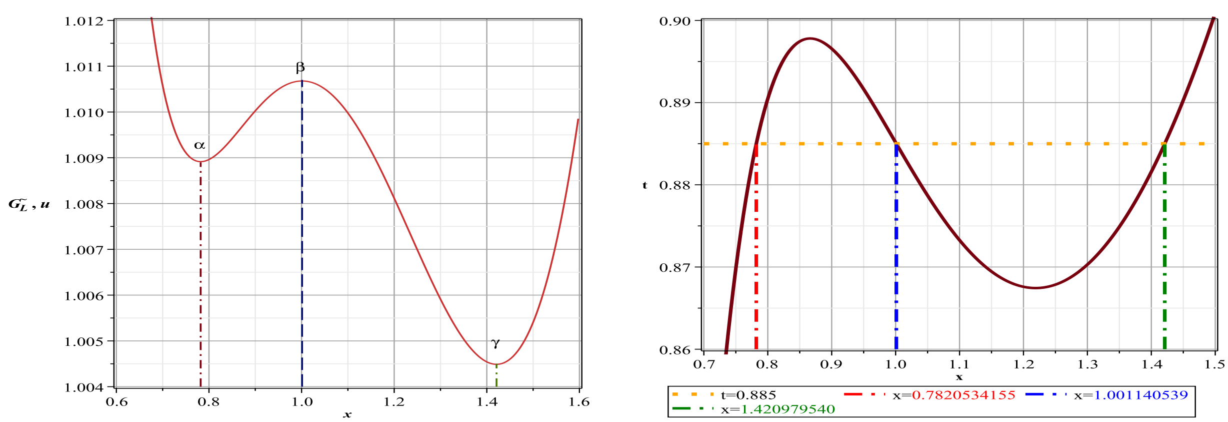

(a) (b)

Figure 5: The graph of G_L against x for free parameters in fig (5a) and T versus x in fig (5b) which are determined as the locations of (α) intersection (red and orange), (β) intersection (blue and orange) and (γ) intersection (green and orange)

Now, using equation (1), we calculate the escape rate of each of the possible transitions, i.e. ($\alpha \rightarrow \beta$) and ($\gamma \rightarrow \beta$), the result of which can be seen in figure (6).

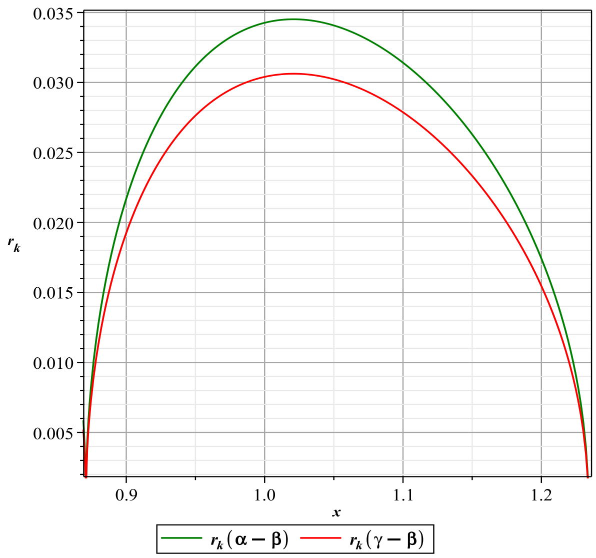

(a)

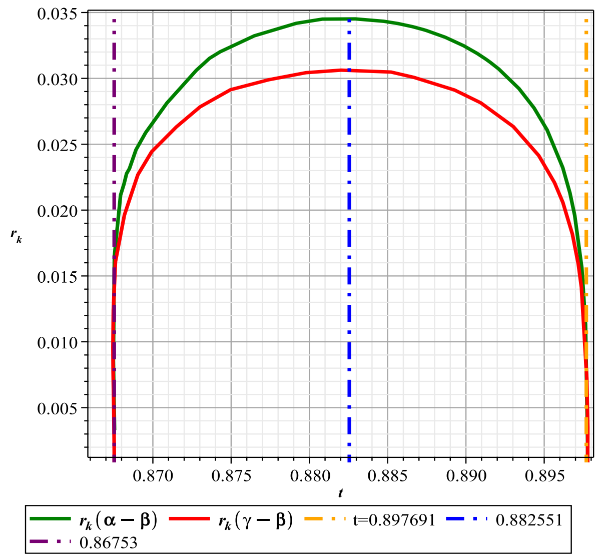

(b)

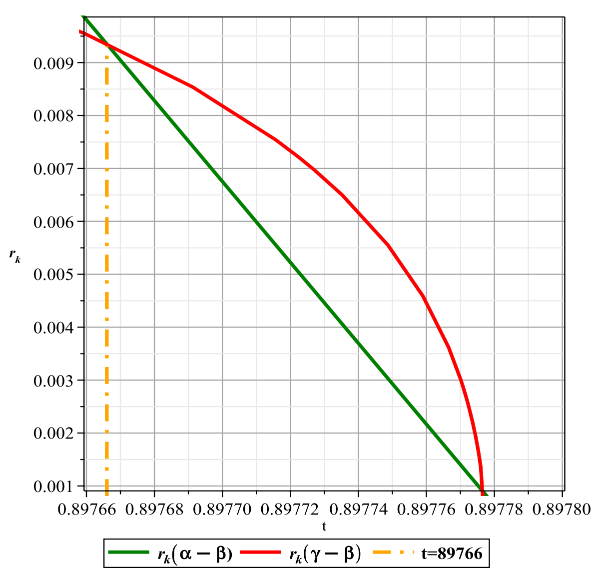

(c)

Figure 6: (6a): r_k with respect to x, (6b): r_k with respect to t and (6c): Enlarged detail, bottom part of diagram (6b)

In Figure 6a, we have plotted the escape rate as a function of distance. For a better interpretation of this graph, it is advisable to read it concurrently with the energy versus distance graph fig (5a). Initially, as energy increases from α towards β, we should witness an increase in the escape growth, which, as confirmed by both figures, should peak at a distance of 1.014. Then, with a gradual decrease in energy from β towards γ, we should observe

a decreasing trend in the probability. Considering the relatively significant height difference between $\gamma \to \beta$ and $\alpha \to \beta$, we expect that throughout the entire range studied, the dominant process should always be the transition from a small to a large black hole, which the graph precisely confirms our classical understanding.
In Figure 6b, we have depicted the escape rate as a function of temperature t. At first glance, the process appears similar to the previous case; that is, initially, with an increase in temperature and considering the small radius, we should observe an increase in the escape rate until it reaches a peak, and then, despite the temperature increase, due to the radius enlargement and energy decrease, we should witness a decreasing trend in probability, which the shape of the graph confirms. However, an analysis of the end section of this graph, which we have illustrated in Figure 6c, reveals that contrary to the previous case, it represents a completely different situation within a small range.
At (t = 0.8976), the two escape rate curves intersect, which, makes their occurrence probabilities equivalent. This means that at this temperature, black holes have the discretion to choose whether to follow the classic process from a small to a large black hole or to undertake a reverse process. Subsequently, it is the reverse process that becomes dominant, meaning that, although this range may seem exceedingly small, the system nonetheless exhibits a propensity within this limited interval to transition from a large black hole to a small black hole, a tendency that may seem contrary to classical expectations.

4 4D AdS Einstein-gauss-bonnet-Yang-Mills black hole with a cloud of strings

Since we tried to explain the contents as much as possible in the previous sections, considering the computational similarities, in this section, we will only mention the basic relationships, and we will bring the similar and unnecessary diagrams in Appendix A. The second selected model is the (EGB-YM-CS) black hole. So the metric of 4D AdS Einstein-gauss-bonnet-yang-mills black hole with a cloud of strings is as follows [64],

$$f(r) = 1 + \frac{r^2\left(1 - \sqrt{1 - 4g\left(\frac{8\pi P}{3} + \frac{q^2}{r^4} - \frac{2M}{r^3} + \frac{a}{r^2}\right)}\right)}{2g}.$$

For the main quantities of this model i.e. mass M, Hawking temperature T_H, entropy S, pressure P and volume V we will have [64],

$$M = \frac{8r^4P\pi + (3a+3)\,r^2 + 3q^2 + 3g}{6r}, \tag{19}$$

$$T_H = \frac{8r^4P\pi + r^2\,(a+1) - q^2 - g}{4\,(r^2+2g)\,r\pi}, \tag{20}$$

$$S = r^2\pi + 4\ln(r)\,g\pi, \tag{21}$$

$$P = \frac{4\pi T\,r^3 + 8\pi Tgr - r^2a + q^2 - r^2 + g}{8r^4\pi}, \tag{22}$$

$$V=\frac{4\pi r^3}{3}, \tag{23}$$

where q is the charge of the black hole, "a" is related to the density of clouds of strings and comes from the energy-momentum tensor of the clouds of strings and g, which is displayed with g instead of α to avoid mistakes with clouds of strings parameter, is a positive Gauss-Bonnet coupling constant.

4.0.1 The landscape free energy

According to equations (2), (3), (4) and (7) for Gibbs and Landau free energy function and thermal potential of this model, we will have,

$$\mathbf{G}=\frac{4P\pi r^3}{3}+\frac{ar}{2}+\frac{g}{2r}+\frac{r}{2}+\frac{q^2}{2r}+\frac{\left(-8r^4P\pi-r^2\left(a+1\right)+q^2+g\right)\left(4\left(\frac{2(r-1)}{r+1}+\frac{2(r-1)^3}{3(r+1)^3}\right)g+r^2\right)}{4\left(r^2+2g\right)r}, \tag{24}$$

$$G_L=\frac{4P\pi r^3}{3}+\frac{ar}{2}+\frac{g}{2r}+\frac{r}{2}+\frac{q^2}{2r}-\left(4g\ln(r)+r^2\right)T\pi, \tag{25}$$

$$\mathbf{U}=\frac{8r^4P\pi+\left(3a+3\right)r^2+3q^2+3g}{6r}-\left(r^2\pi+4\ln(r)\,g\pi\right)T, \tag{26}$$

$$\mathbf{L}=PX-\frac{2\,6^{\frac{2}{3}}\left(-\frac{3\pi^{\frac{1}{3}}6^{\frac{2}{3}}(a+1)X^{\frac{2}{3}}}{16}+\pi^{\frac{5}{3}}Tg6^{\frac{1}{3}}\ln(X)\,X^{\frac{1}{3}}+\frac{9\pi\left(TX-\frac{2q^2}{3}-\frac{2g}{3}\right)}{8}\right)}{9\pi^{\frac{2}{3}}X^{\frac{1}{3}}}, \tag{27}$$

Now we will go to a special state that is formed based on the arbitrary parameter setting. For this purpose, by considering the values $a=1.5, q=0.5, g=0.5$ for the parameters and with a little calculation for the critical quantities, we will have,

$$\begin{aligned} &T_c=0.0978, \qquad P_c=0.0075, \qquad r_c=2.269260985,\\ &V_c=48.94878867, \qquad U_c=1.28320692868, \qquad G_c=1.28662690146, \end{aligned} \tag{28}$$

In this model, we still use relations (17) to make the equations dimensionless.

4.0.2 Kramer's escape rate

In this black hole, unlike the previous case where we examined a specific state of the potential of the system at a certain pressure in terms of temperature changes, we are looking to investigate the changes in the rate of escape, at a constant temperature for a certain state of the system, in terms of pressure. For this purpose, we consider the temperature t = 0.937, which is equivalent to the energy state of the system in Fig (7a).

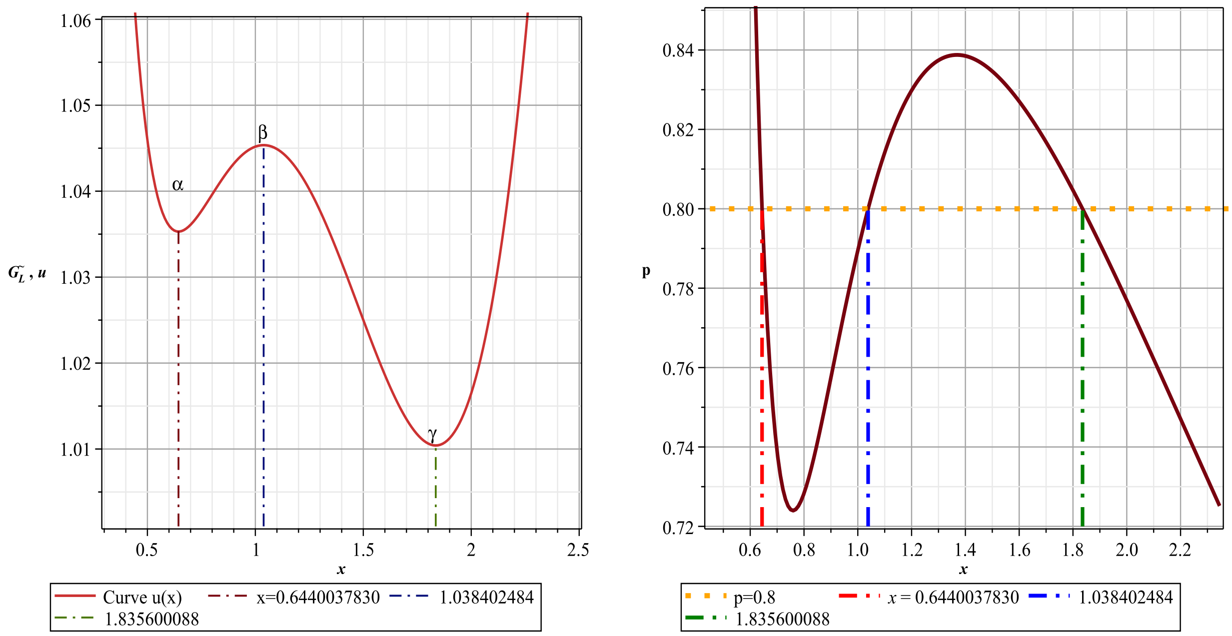

(a)

(b)

Figure 7: The graph of G_L against x for free parameters in fig (7a) and p versus x in fig (7b) which are determined as the locations of (α) intersection (red and orange), (β) intersection (blue and orange) and (γ) intersection (green and orange)

Now, using equation (1), we calculate the escape rate of each of the possible transitions, i.e. ($\alpha \rightarrow \beta$) and ($\gamma \rightarrow \beta$), the result of which can be seen in fig (8).

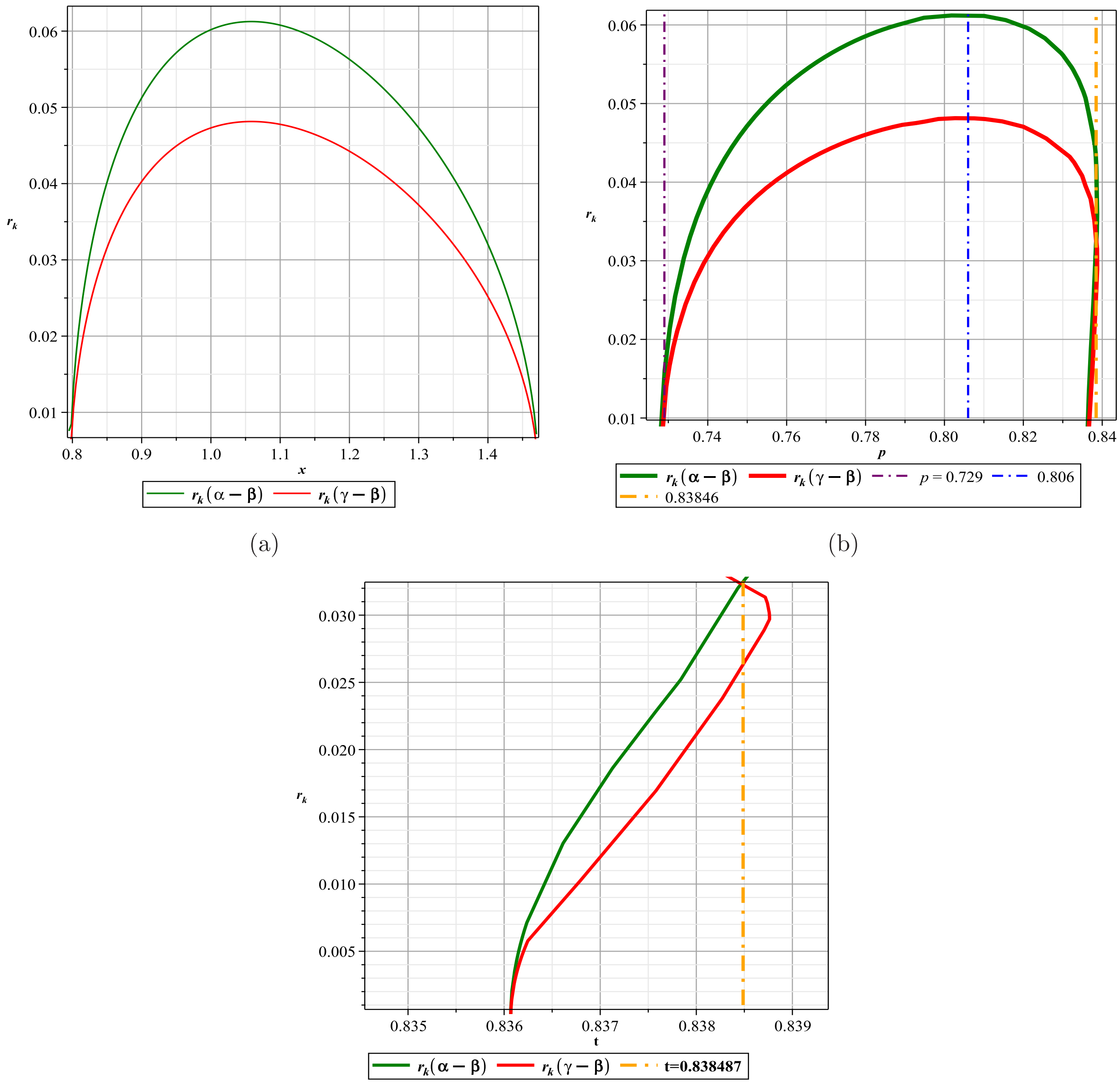

(a) (b)

(c)

Figure 8: (8a): r_k with respect to x, (8b): r_k with respect to p and (8c): Enlarged detail, bottom part of diagram (8b)

As it is evident from Fig (8c), at (p = 0.8384), again the two escape rate curves intersect, which makes their occurrence probabilities equivalent. It appears that after this convergence point, a process entirely different from the nonlinear or charged model takes shape. This means that quantitatively, the pressure associated with the transition from a large black hole to a small one increases more than in the reverse case. However, this increase in pressure for the transition from a large to a small black hole does not actually cause the corresponding probability to increase as well, leading not to the dominance of the large to small black hole trend. As can be seen from the figure, if we draw an isobar, we find that r_{k1} remains larger than r_{k2}. This may indicate a greater harmony and alignment of this model with the known natural laws of physics

5 Discussion and comparison

In this section, for a better understanding, comparison, and interpretation of the results, it is first beneficial to delve a little into the concept of transition from small to large black holes (or large to small). The transition from a small to a large black hole can generally occur through the accretion of matter and energy from the surrounding environment of the black hole, or it can also occur through the merging of black holes, which may be accompanied by intensified emission of gravitational waves. However, from a thermodynamic perspective, this transition seems to encompass any physical process that facilitates changes in temperature, pressure, and other thermodynamic parameters in such a way that it leads to an increase in the radius of the event horizon and consequently, the enlargement of the black hole, which, given the super-gravitational structure of black holes, is a highly probable process. The reverse process, the transition from a large to a small black hole, can occur through processes such as Hawking radiation, where black holes emit particles due to quantum effects near the event horizon. Over time, this radiation can lead to a reduction in the mass and size of the black hole and its eventual evaporation. From a thermodynamic perspective, this phenomenon is equivalent to any process that creates a change in thermodynamic parameters leading to a reduction in the radius of the horizon and the shrinking of the black hole.

As observed in Figs (5a) and (7a), our black hole initially resides in a stable local minimum, alpha, which globally is considered an unstable minimum. Consequently, as one would naturally expect, with the slightest thermal perturbation, and corresponding pressure, the system increasingly tends to transition towards the global minimum,γ, signifying an increase in radius. As the radius increases and the system begins to move towards a larger black hole, according to the reaction principle, it is natural that processes that prevent excessive radial growth and uncontrolled instability also form. This leads to the fact that the escape rate after reaching a peak, a decreasing trend will ensue, and the system will potentially stabilize at the global minimum (Fig (6c)).

However, in (NLM-C-Q-PFD) modle, when examining the escape rate diagram as a function of temperature (or pressure), we find that when the temperature (and corresponding pressure) exceeds a certain limit, a small range emerges where a reverse process forms and prevails Fig (6c). In other words, With r_{k2} prevailing over r_{k1}, a situation is created that allows black holes to move from γ to β. It seems that the transition from γ to β is less consistent with physical conditions. This is because, within the same energy structure and without topological changes in the energy function (that is, maintaining the gamma state as the global minimum and alpha as the local minimum), the system prefers to reach an α state with a smaller radius and consequently reduced entropy, which is at a higher energetic level. Therefore, from our perspective, this situation can be termed 'low probable.'

In our opinion, based on the results, it appears that the larger this region is, meaning the reverse process begins at lower temperatures or pressures, it may indicate an incomplete structural evolution of the black hole model to fully conform with the laws of nature. For example, in the Reissner-Nordstrm black hole [48], as a basic model that includes only electric charge, this region is significantly larger and practically quite evident. As we know, due to the choice of mass and charge size, this model has repeatedly shown non-conformity with standard physical conditions and cosmological conjectures [61,62]. In other words, from comparing the results of the Reissner-Nordstrm model with the (NLM-C-Q-PFD) black hole, it seems that the addition of parameters influenced by dark structure (energy and matter) has led to the black hole behavior approaching a more natural and orderly structure. The situation regarding the (EGB-YM-CS) structure is completely different from the previous state. It appears that after the convergence point of the two probability diagrams, which gives black holes an equal choice to move between two minima, the transition from γ to β, in terms of increasing pressure changes, overtakes the transition from α to β. However, this increase in pressure, according to diagram (8c), is not accompanied by an increased probability of transition; that is, if we draw an isobar in any region after the convergence, we will see that the transition probability r_{k1} remains greater than r_{k2} . It seems that the transition from α to β after the convergence point, with decreasing pressure, prevents the 'low probable' process and displays a complete harmony with nature.

6 Conclusion

The study of black hole phase transitions based on the Gibbs free energy function is an important and influential part of advancing our understanding of black hole thermodynamics. However, a point that existed in this conventional method was that it seemed only static phase transitions were considered, leaving questions about the dynamics of phase transitions unanswered.

The proposition that the dynamics of phase transitions in black holes are controlled by thermodynamic and statistical forces, followed by the study of phase transitions according to the stochastic Langevin equation or the Fokker-Planck equation [33], and considering the 'mean first passage time' in some studies [34–56], and then the introduction of Kramer's escape rate in the study of phase transitions [60], motivated us to examine and compare different forms of the free energy landscape and then study Kramer's escape rate in the first-order phase transitions of more complex black holes. These black holes are specifically formed based on cosmic and stringy properties, meaning they interact more with the features of dark structures. Our goal is to see what similarities or differences the addition of dark structure and stringy parameters create in the behavior of these black holes compared to the simpler model of the charged black hole.

According to this, in this article, we examined the escape rate from two perspectives. Initially, we considered it in terms of distance or the radius of the black hole and observed that black holes exhibit natural behavior consistent with environmental evidence. That is, the escape rate initially increases with the radius until it reaches a certain maximum, but this increase is not uncontrolled or permanent. A physical feedback mechanism causes this probability to gradually decrease, ending at a specific radius tolerable for the black hole's survival. What is evident in comparison is that the escape rate and leakage from the small to the large black hole always dominate over the reverse. However,in the (NLM-C-Q-PFD) case, the escape rate diagram as a function of temperature (pressure) indicates something else. Meaning that the diagram initially, at its peak, and even near the end, shows behavior similar to the escape rate diagram as a function of distance. But suddenly, near the end, at a relatively high temperature (pressure), it takes on a different behavior. Specifically, at a certain temperature (pressure), the probability of transitioning from small to large and vice versa becomes equal. This implies that at this temperature, black holes have the 'choice' to select their desired path towards either the small or large black hole. After this temperature, in a region, albeit small, the process completely reverses, meaning the probability of transitioning from the large to the small black hole becomes dominant, and black holes prefer to take the path from the large to the small black hole! But in the case of (EGB-YM-CS), after the intersection point of the graphs, the high probable transition still maintains its preference over the 'low probable' transition and, in our opinion, shows a more perfect harmony with nature.We have addressed this in the discussion and comparison section. What we found in comparison with the charged black hole model is that in the charged model, this region is quite evident and noticeable. However, with the addition of parameters related to dark structure, this region-which we consider to be less physical-will either disappear (EGB-YM-CS) or become so small that radial changes due to their insignificance do not appear in the radius diagram, but still exist in the escape rate diagram (NLM-C-Q-PFD) as a function of temperature (pressure). The question of whether the existence of this region, albeit small, for a black hole has a physical interpretation and is considered natural behavior, and how it should be justified, is something that requires further study of various models. However, in conclusion, it seems that as the theoretical models of black holes evolve and more empirical and observable factors such as dark structure are added to the model, there will exist greater conformity with the 'pattern of repetition' mentioned at the beginning of the introduction.

7 Appendix A: Behavioral sequence of the free energy landscape for (EGB-YM-CS) black hole

The swallow tail representation of the Gibbs free energy landscape in terms of t and the behavioral sequence of the potential function in terms of distance and temperature for the (EGB-YM-CS) black hole is shown in Fig (10), (11).

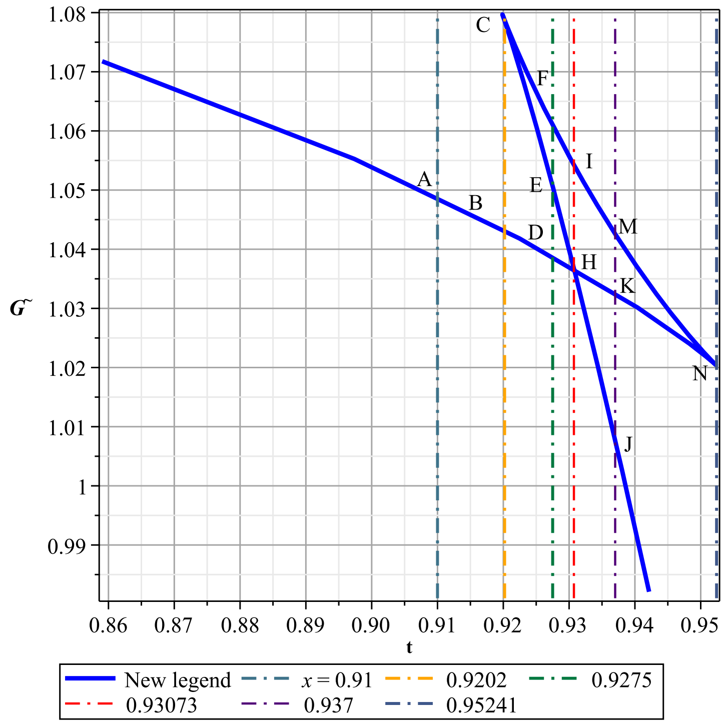

Figure 9: The Gibbs free energy landscape in terms of t

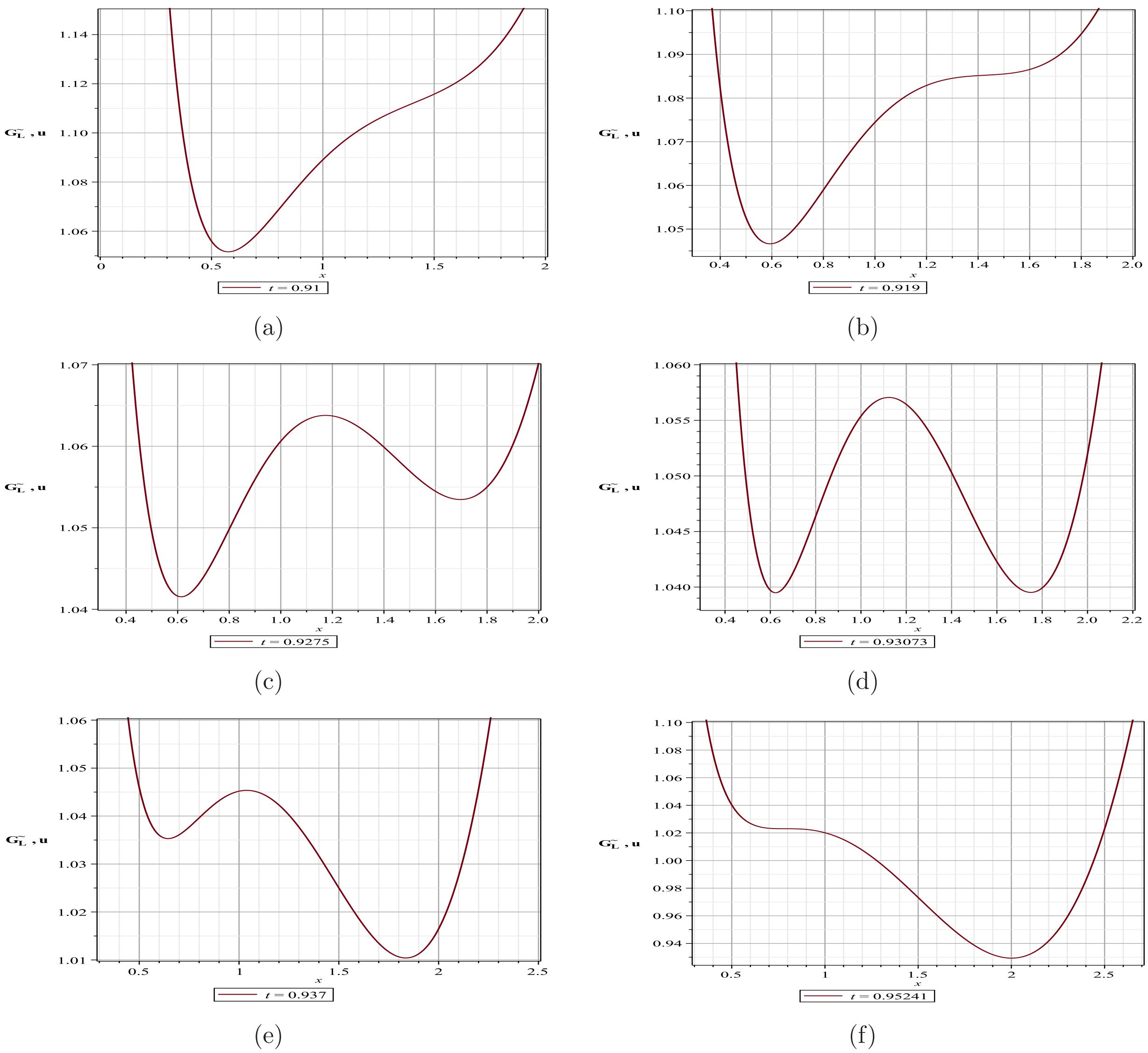

Figure 10: Behavioral sequence of energy in terms of x for different temperatures

References

[1] Hawking, Stephen W. "Particle creation by black holes." Communications in mathematical physics 43.3 (1975): 199-220.

[2] Bekenstein, Jacob D. "Black holes and the second law." JACOB BEKENSTEIN: The Conservative Revolutionary. 2020. 303-306.

[3] Bekenstein, Jacob D. "Black holes and entropy." Physical Review D 7.8 (1973): 2333.

[4] Bardeen, James M., Brandon Carter, and Stephen W. Hawking. "The four laws of black hole mechanics." Communications in mathematical physics 31 (1973): 161-170.

[5] Kastor, David, Sourya Ray, and Jennie Traschen. "Enthalpy and the mechanics of AdS black holes." Classical and Quantum Gravity 26.19 (2009): 195011.

[6] Chamblin, Andrew, et al. "Charged AdS black holes and catastrophic holography." Physical Review D 60.6 (1999): 064018.

[7] Chamblin, Andrew, et al. "Holography, thermodynamics, and fluctuations of charged AdS black holes." Physical Review D 60.10 (1999): 104026.

[8] Caldarelli, Marco M., Guido Cognola, and Dietmar Klemm. "Thermodynamics of Kerr-Newman-AdS black holes and conformal field theories." Classical and Quantum Gravity 17.2 (2000): 399.

[9] Dolan, Brian P. "The cosmological constant and the black hole equation of state." arXiv preprint arXiv:1008.5023 (2010).

[10] B. P. Dolan, Pressure and volume in the first law of black hole thermodynamics, Class.Quant. Grav. 28, 235017 (2011).

[11] Kubiznak, David, and Robert B. Mann. "P-V criticality of charged AdS black holes." Journal of High Energy Physics 2012.7 (2012): 1-25.

[12] Hawking, Stephen W., and Don N. Page. "Thermodynamics of black holes in anti-de Sitter space." Communications in Mathematical Physics 87 (1983): 577-588.

[13] Hendi, S. H., and M. H. Vahidinia. "Extended phase space thermodynamics and P-V criticality of black holes with a nonlinear source." Physical Review D 88.8 (2013): 084045.

[14] Bhattacharya, Krishnakanta, Bibhas Ranjan Majhi, and Saurav Samanta. "Van der Waals criticality in AdS black holes: a phenomenological study." Physical Review D 96.8 (2017): 084037.

[15] Cai, Rong-Gen. "Gauss-Bonnet black holes in AdS spaces." Physical Review D 65.8 (2002): 084014.

[16] Majhi, Bibhas Ranjan, and Saurav Samanta. "PV criticality of AdS black holes in a general framework." Physics Letters B 773 (2017): 203-207.

[17] Sadeghi, Jafar, et al. "Thermodynamic topology and photon spheres in the hyperscaling violating black holes." Astroparticle Physics 156 (2024): 102920.

[18] Sadeghi, J., et al. "Topology of Hayward-AdS black hole thermodynamics." Physica Scripta 99.2 (2024): 025003.

[19] Wu, Di, and Shuang-Qing Wu. "Topological classes of thermodynamics of rotating AdS black holes." Physical Review D 107.8 (2023): 084002.

[20] Wu, Di. "Topological classes of thermodynamics of the four-dimensional static accelerating black holes." Physical Review D 108.8 (2023): 084041.

[21] Sadeghi, Jafar, et al. "Thermodynamic topology of black holes from bulk-boundary, extended, and restricted phase space perspectives." Annals of Physics 460 (2024): 169569.

[22] Wu, Di. "Topological classes of rotating black holes." Physical Review D 107.2 (2023): 024024.

[23] Alipour, Mohammad Reza, et al. "Topological classification and black hole thermodynamics." Physics of the Dark Universe 42 (2023): 101361.

[24] Sadeghi, Jafar, et al. "Bardeen black hole thermodynamics from topological perspective." Annals of Physics 455 (2023): 169391.

[25] Sadeghi, Jafar, et al. "Bulk-boundary and RPS Thermodynamics from Topology perspective." arXiv preprint arXiv:2306.16117 (2023).

[26] Wei, Shao-Wen, Yu-Xiao Liu, and Robert B. Mann. "Black hole solutions as topological thermodynamic defects." Physical Review Letters 129.19 (2022): 191101.

[27] Zhang, Ming, and Jie Jiang. "Bulk-boundary thermodynamic equivalence: a topology viewpoint." Journal of High Energy Physics 2023.6 (2023): 1-17.

[28] Hazarika, Bidyut, and Prabwal Phukon. "Thermodynamic topology of black holes in f (R) gravity." Progress of Theoretical and Experimental Physics 2024.4 (2024): 043E01.

[29] Lee, Chi-Lun, et al. "Diffusion dynamics, moments, and distribution of first-passage time on the protein-folding energy landscape, with applications to single molecules." Physical Review E 67.4 (2003): 041905.

[30] Lee, Chi-Lun, George Stell, and Jin Wang. "First-passage time distribution and non-Markovian diffusion dynamics of protein folding." The Journal of chemical physics 118.2 (2003): 959-968.

[31] Wang, Jin. "Landscape and flux theory of non-equilibrium dynamical systems with application to biology." Advances in Physics 64.1 (2015): 1-137.

[32] Bryngelson, Joseph D., and Peter G. Wolynes. "Intermediates and barrier crossing in a random energy model (with applications to protein folding)." The Journal of Physical Chemistry 93.19 (1989): 6902-6915.

[33] Li, Ran, Kun Zhang, and Jin Wang. "Thermal dynamic phase transition of Reissner-Nordström Anti-de Sitter black holes on free energy landscape." Journal of High Energy Physics 2020.10 (2020): 1-25.

[34] Li, Ran, Kun Zhang, and Jin Wang. "Probing black hole microstructure with the kinetic turnover of phase transition." Physical Review D 104.8 (2021): 084076.

[35] Li, Ran, Kun Zhang, and Jin Wang. "Thermal dynamic phase transition of Reissner-Nordström Anti-de Sitter black holes on free energy landscape." Journal of High Energy Physics 2020.10 (2020): 1-25.

[36] Mo, Jie-Xiong, and Shan-Quan Lan. "Dynamic phase transition of charged dilaton black holes." Chinese Physics C 45.10 (2021): 105106.

[37] Du, Yun-Zhi, et al. "Dynamic property of phase transition for non-linear charged anti-de Sitter black holes." Chinese Physics C 46.5 (2022): 055104.

[38] Yang, Si-Jiang, et al. "Kinetics of a phase transition for a Kerr-AdS black hole on the free-energy landscape." Physical Review D 105.8 (2022): 084030.

[39] Kumara, A. Naveena, et al. "Dynamics and kinetics of phase transition for regular AdS black holes in general relativity coupled to nonlinear electrodynamics." International Journal of Modern Physics A 38.29n30 (2023): 2350151.

[40] Lan, Shan-Quan, et al. "Effects of dark energy on dynamic phase transition of charged AdS black holes." Physical Review D 104.10 (2021): 104032.

[41] Li, Ran, and Jin Wang. "Free energy landscape and kinetics of phase transition in two coupled SYK models and the corresponding wormhole-two black hole switching." Journal of High Energy Physics 2021.12 (2021): 1-20.

[42] Li, Ran, Kun Zhang, and Jin Wang. "Probing black hole microstructure with the kinetic turnover of phase transition." Physical Review D 104.8 (2021): 084076.

[43] Li, Ran, Kun Zhang, and Jin Wang. "Kinetics and its turnover of Hawking-Page phase transition under the black hole evaporation." Physical Review D 104.8 (2021): 084060.

[44] Luo, Zhi, Hao Yu, and Jin Li. "Effects of a global monopole on the thermodynamic phase transition of a charged AdS black hole." Chinese Physics C 46.12 (2022): 125101.

[45] Li, Ran, and Jin Wang. "Generalized free energy landscape of a black hole phase transition." Physical Review D 106.10 (2022): 106015.

[46] Yang, Si-Jiang, et al. "Kinetics of a phase transition for a Kerr-AdS black hole on the free-energy landscape." Physical Review D 105.8 (2022): 084030.

[47] Li, Ran, and Jin Wang. "Kinetics of Hawking-Page phase transition with the non-Markovian effects." Journal of High Energy Physics 2022.5 (2022): 1-25.

[48] Li, Ran, and Jin Wang. "Non-Markovian dynamics of black hole phase transition." Physical Review D 106.10 (2022): 104039.

[49] Liu, Conghua, and Jin Wang. "Path integral and instantons for the dynamical process and phase transition rate of Reissner-Nordström-AdS black holes." Physical Review D 105.10 (2022): 104024.

[50] Ali, Md Sabir, et al. "Born-Infeld-AdS black hole phase structure: Landau theory and free energy landscape approaches." arXiv preprint arXiv:2303.11711 (2023).

[51] Yang, Jiayue, and Robert B. Mann. "Dynamic behaviours of black hole phase transitions near quadruple points." Journal of High Energy Physics 2023.8 (2023): 1-21.

[52] Safir, T. K., et al. "Dynamic phase transition of black holes in massive gravity." Annals of Physics 458 (2023): 169480.

[53] Liu, Conghua, et al. "Generalized free energy and dynamical state transition of the dyonic AdS black hole in the grand canonical ensemble." Journal of High Energy Physics 2023.11 (2023): 1-33.

[54] Li, Ran, and Jin Wang. "Generalized free energy landscapes of charged Gauss-Bonnet-AdS black holes in diverse dimensions." Physical Review D 108.4 (2023): 044057.

[55] Dai, Heng, Zixu Zhao, and Shuhang Zhang. "Thermodynamic phase transition of Euler-Heisenberg-AdS black hole on free energy landscape." Nuclear Physics B 991 (2023): 116219.

[56] Li, Ran, Conghua Liu, and Jin Wang. "Phase space path integral approach to the kinetics of black hole phase transition." arXiv preprint arXiv:2401.02260 (2024).

[57] Xu, Zhen-Ming, Bin Wu, and Wen-Li Yang. "van der Waals fluid and charged AdS black hole in the Landau theory." Classical and Quantum Gravity 38.20 (2021): 205008.

[58] Ali, Md Sabir, et al. "Born-Infeld-AdS black hole phase structure: Landau theory and free energy landscape approaches." arXiv preprint arXiv:2303.11711 (2023).

[59] Xu, Zhen-Ming. "Fokker-Planck equation for black holes in thermal potential." Physical Review D 104.10 (2021): 104022.

[60] Xu, Zhen-Ming, Bin Wu, and Wen-Li Yang. "Rate of the phase transition for a charged anti-de Sitter black hole." Science China Physics, Mechanics Astronomy 66.4 (2023): 240411.

[61] Wang, Yu-Shan, Zhen-Ming Xu, and Bin Wu. "Thermodynamic phase transition rate for the third-order Lovelock black hole in diverse dimensions." arXiv preprint arXiv:2402.08887 (2024).

[62] Du, Yun-Zhi, et al. "Topology and phase transition for EPYM AdS black hole in thermal potential." arXiv preprint arXiv:2309.00224 (2023).

[63] Ndongmo, Ragil, et al. "Thermodynamics of Non-linear magnetic-charged AdS black hole surrounded by quintessence, in the background of perfect fluid dark matter." Physics of the Dark Universe 42 (2023): 101299.

[64] Rahmani, Faramarz, and Mehdi Sadeghi. "The Phase Transition of $4D$ Yang-Mills Charged GB AdS Black Hole with Cloud of Strings." arXiv preprint arXiv:2402.07856 (2024).

[65] Berera, Arjun, et al. "Formulating the Kramers problem in field theory." Physical Review D 100.7 (2019): 076005.

[66] Zhou, Yanjun, and Jiulin Du. "Escape rate for the power-law distribution in low-to-intermediate damping." Physica A: Statistical Mechanics and its Applications 403 (2014): 244-251.

[67] Zhou, Yanjun, and Jiulin Du. "Kramers escape rate in overdamped systems with the power-law distribution." Physica A: Statistical Mechanics and its Applications 402 (2014): 299-305.

[68] H. Risken and T. Frank, The Fokker-Planck Equation:Methods of Solution and Applications (Springer-Verlag,Berlin, Germany, 1996)

[69] Talkner, Peter. "Mean first passage time and the lifetime of a metastable state." Zeitschrift für Physik B Condensed Matter 68.2 (1987): 201-207.

[70] Van Kampen, Nicolaas Godfried. Stochastic processes in physics and chemistry. Vol. 1. Elsevier, 1992.

[71] Abhishek Dhar, Lecture note'Kramer s escape rate across a barrier', https://home.icts.res.in/ abhi/notes/kram.pdf

[72] Wei, Shao-Wen, Yu-Xiao Liu, and Yong-Qiang Wang. "Dynamic properties of thermodynamic phase transition for five-dimensional neutral Gauss-Bonnet AdS black hole on free energy landscape." Nuclear Physics B 976 (2022): 115692.

[73] Penrose, Roger. "Gravitational collapse and space-time singularities." Physical Review Letters 14.3 (1965): 57.

[74] Shaymatov, Sanjar, Bobomurat Ahmedov, and Mubasher Jamil. "Testing the weak cosmic censorship conjecture for a Reissner–Nordström–de Sitter black hole surrounded by perfect fluid dark matter." The European Physical Journal C 81 (2021): 1-11.